

Online b -jets tagging at CDFS.Amerio*, M.Casarsa[†], G.Cortiana*, D.Lucchesi*, S.Pagan Griso* L.Ristori[‡] and S.Torre[§]

*University of Padova and INFN

[†]Fermilab[‡]INFN Pisa[§]INFN/LNF Frascati

Abstract—We propose a method to identify b -quark jets at trigger level which exploits recently increased CDF trigger system capabilities. b -quark jets identification is of central interest for the CDF high- P_T physics program, and the possibility to select online b -jets enriched samples can extend the physics reaches especially for light Higgs boson searches where the $H \rightarrow b\bar{b}$ decay mode is dominant. Exploiting new trigger primitives provided by two recent trigger upgrades, the Level2 XFT stereo tracking [1] and the improved Level2 cluster-finder [2], in conjunction with the existing Silicon Vertex Tracker (SVT) [3] [4], we design an online trigger algorithm aimed at selecting good purity b -jets samples useful for many physics measurements, the most important being inclusive $H \rightarrow b\bar{b}$ searches. We discuss the performances of the proposed b -tagging algorithm which must guarantee reasonable trigger rates at luminosity greater than $2 \times 10^{32} \text{ cm}^{-2} \text{ s}^{-1}$ and provide high efficiency on $H \rightarrow b\bar{b}$ events.

I. PHYSICS MOTIVATION

The selection of events enriched of b -jets is of fundamental importance in the study of many physics processes but it suffers for a large background from light QCD events. The possibility of trigger on these events could greatly improve purity of b -jet samples.

Since Tevatron luminosity has increased above $1.5 \times 10^{32} \text{ cm}^{-2} \text{ s}^{-1}$, existing b -jet triggers suffer from very high rates and thus have to be prescaled and/or enabled only when the luminosity goes below a given threshold. This way of keeping rate under control suffers the big drawback of an efficiency loss on signal. In order to overcome this obstacle, we propose a new trigger able to select b -jets final states up to luminosity greater than $2.0 \times 10^{32} \text{ cm}^{-2} \text{ s}^{-1}$.

This trigger is optimized with respect to $H \rightarrow b\bar{b}$, which is the dominant decay mode for a light Higgs boson, but aims at having a good efficiency also on $Z \rightarrow b\bar{b}$ channel, important for b -jet energy scale measurement and as a normalization channel for inclusive $H \rightarrow b\bar{b}$ searches.

A trigger having good efficiency on b -jets final states can also extend the physics reach for neutral MSSM Higgs $\phi \rightarrow b\bar{b}$: according to MSSM, this channel has $BR \sim 90\%$, but overwhelming dijet and multijet backgrounds make any search of this signal very difficult.

In the following, we will first review the CDF detector, its trigger system and the upgrades currently under commissioning for high luminosity data taking. We will then illustrate our proposal for a b -jet trigger optimized to have high efficiency on $H \rightarrow b\bar{b}$ events while maintaining acceptable rate at high luminosity. The effect on $Z \rightarrow b\bar{b}$ events is also discussed.

II. CDF DETECTOR

CDF is an azimuthally and forward-backward symmetric detector. It consists of a charged-particle tracking system immersed in a 1.4 T magnetic field followed by calorimeters which are surrounded by muon detectors. A detailed description can be found in [5].

The CDF II coordinate system uses θ and ϕ as the polar and azimuthal angles, respectively, defined with respect to the proton beam axis direction, z . The pseudo-rapidity η is defined as $\eta \equiv -\ln[\tan(\theta/2)]$. The transverse momentum of a particle is $p_T = p \sin \theta$ and the transverse energy is defined as $E_T = E \sin \theta$.

The parts of the detector relevant for our trigger studies are tracking and calorimetric systems. The first consists of a 8-layer silicon microstrip detector and a drift chamber providing η coverage up to 2.0 and 1.0 respectively. Calorimeters consist of projective towers with electromagnetic and hadronic sections covering the region up to $|\eta| < 3.6$.

A. CDF Trigger System

CDF trigger is a three level system [6] designed to reduce the bunch crossing rate of 1.7 MHz to approximately 100 Hz, the current limit to write to tape. At Level-1 (L1) raw muons, tracks and calorimeter information are processed to produce a L1 decision. L1 is a synchronous 40 stages pipeline and it is based on custom-designed hardware. It can provide a trigger decision in $5.5 \mu\text{s}$. When an event is accepted at L1, subsets of detector information are sent to the Level-2 (L2) system, where some limited event reconstruction is performed and a L2 decision is taken. L2 is an asynchronous pipeline and it is based on a combination of custom-designed hardware and commodity processors. Its average latency is $20 \mu\text{s}$ and its maximum output rate is 300 Hz. Upon L2 accept, the full detector data is readout and sent to Level-3 (L3) processor farm for further processing. Events accepted at L3 are sent to mass storage. L3 maximum output rate is ~ 100 Hz.

B. Upgrades

The increase in Tevatron luminosity has forced CDF collaboration to cope with increasing trigger rates. In order to meet the new requirements, many subsystem of CDF trigger system had to be upgraded. The upgrades, while helping in keeping trigger rates under control, can provide new tools to be used in the design of innovative triggers. In the following,

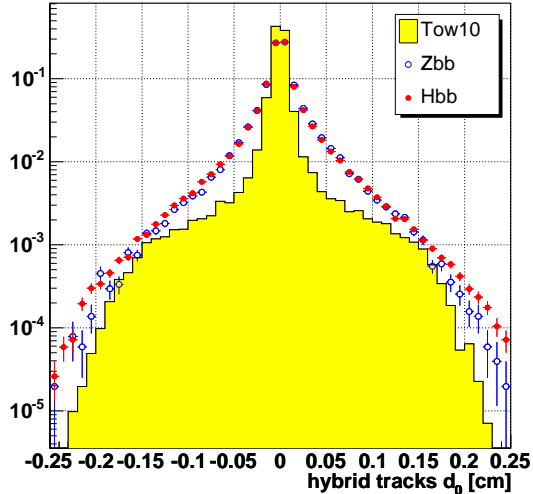


Fig. 1. Impact parameter distribution for tracks matching L2 cones.

we will give a brief description of the upgrades we exploit for the implementation of online b -tagging.

1) *XFT upgrade*: The Extremely Fast Tracker (XFT) [1] has been developed to find tracks in the transverse plane of the drift chamber in time for L1 decision, using hit data from the 4 *axial* superlayers of the chamber. XFT can measure transverse momentum and azimuthal angle ϕ of all the tracks with $p_T > 1.5$ GeV/c with an efficiency greater than 96% and a resolution $\sigma_{p_T}/P_T^2 \sim 2\%$ (GeV^{-1}) and $\sigma_\phi \sim 6$ mrad. The upgraded system can now reject at L1 fake axial tracks by requiring the association with *stereo* segments. The rejection factor is about 7. Moreover XFT segments of finer granularity can be sent to L2 where a 3D-track reconstruction can be performed with a good resolution on $\cot\theta$ ($\sigma_{\cot\theta} = 0.11$) and z_0 ($\sigma_{z_0} = 11$ cm).

2) *L2 calorimeter trigger upgrade*: The current L2 calorimeter cluster finder looks for energy deposits in electromagnetic and hadronic calorimeters using an algorithm that forms clusters by simply combining contiguous regions of trigger towers with non-trivial energy. This algorithm suffers from large fake rate at high luminosity. The upgraded system will use a new *fixed cone* cluster finding algorithm exploiting full trigger tower energy information. As a consequence, L2 jets nearly equivalent to offline ones will be available, allowing not only a trigger rate reduction but also much more precise measurements of jet energies and directions.

XFT improved tracking capabilities, with the addition of the already available SVT tracker [3] [4], will be combined with improved jet reconstruction in order to perform at L2 an efficient track-cone matching, key element of our b -tagging algorithm.

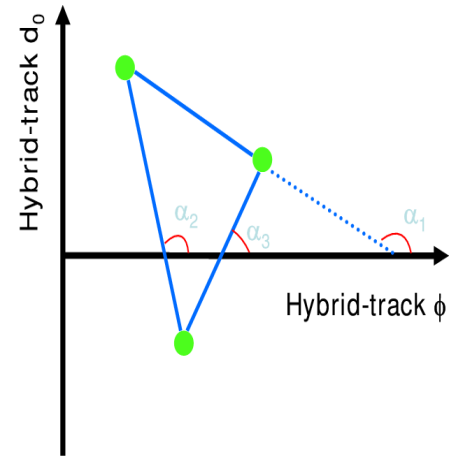


Fig. 2. b -jet tracks in $d_0 - \phi$ plane. The opposite of the slope of each segment joining two tracks is an estimator of b -quark decay length R_b

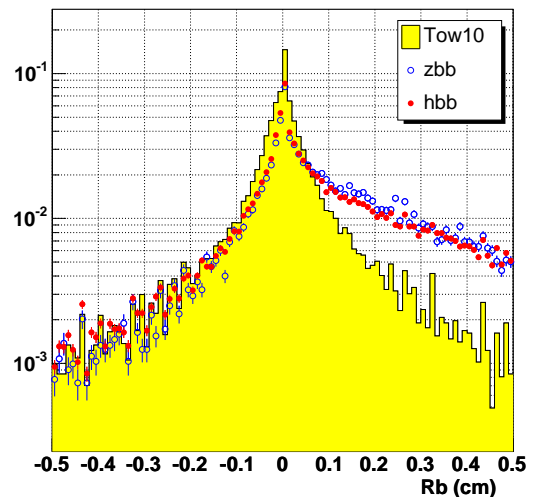


Fig. 3. b -quark decay length (R_b) distribution for tracks matching L2 cones: real b -jets tend to have positive R_b values.

III. TRIGGER ARCHITECTURE

The online b -tagging algorithm we propose is optimized for $H \rightarrow b\bar{b}$ search. During the development of the algorithm, we also monitored its effect on $Z \rightarrow b\bar{b}$ events which are somehow similar.

A $H \rightarrow b\bar{b}$ event has two central jets in the final state, both with high transverse energy. As b quark travels some millimeters before decaying, we expect tracks in b -jet cones to be displaced from the primary vertex. Thus the idea at the basis of our trigger is exploiting the displacement of b -jet tracks while trying to keep cuts on jet energies as much low as possible, in order to limit their effect on dijet invariant

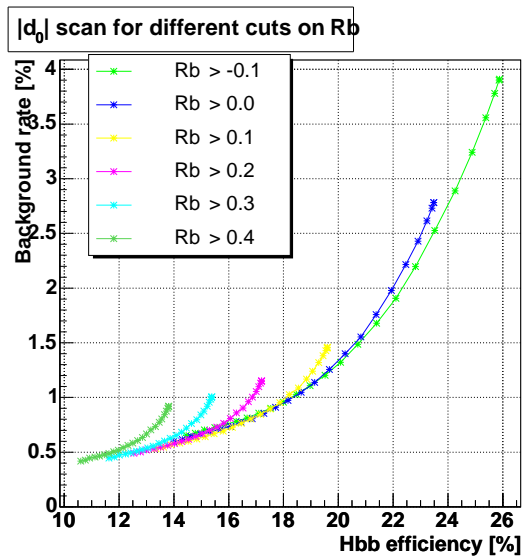


Fig. 4. Background rate VS efficiency on signal for different cuts on R_b and d_0 . Each curve represent a cut on R_b and each point in the curve a cut on $|d_0|$.

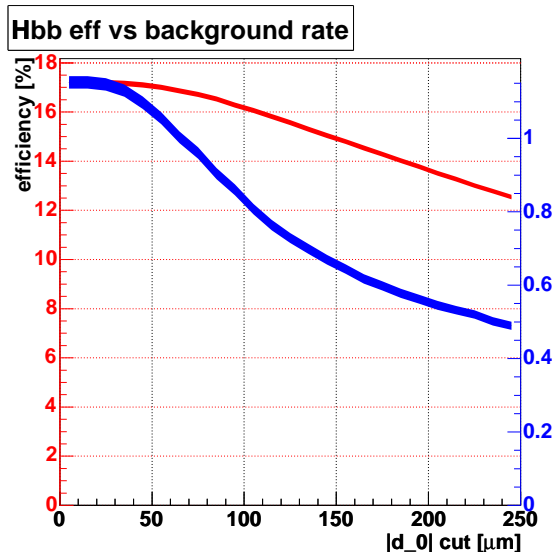


Fig. 5. Efficiency on signal and background varying $|d_0|$ cut on one of the matched tracks.

mass distribution.

The studies that follow are done using Pythia Monte Carlo for $H \rightarrow b\bar{b}$ ($M_H = 120$ GeV) and $Z \rightarrow b\bar{b}$ signals and data for background. Data events are collected by a trigger requiring just one calorimetric trigger tower above 10 GeV at L1 (*Tower10* trigger).

A. L1

A $H \rightarrow b\bar{b}$ event has two high energy jets and at L2, as we shall see, we need one of them matching with at least two tracks. Thus at L1 we require at least one trigger tower with $E_T \geq 10$ GeV and two XFT, stereo confirmed, tracks being contained in the same jet cone. As at L1 we do not have

information about track polar angle, to meet this requirement we can only look at differences in azimuthal angle ϕ , asking $\Delta\phi < 0.7$ rad ($\Delta R = \sqrt{\Delta\eta^2 + \Delta\phi^2} = 0.7$ is L2 jet cone radius in $\eta - \phi$ plane).

B. L2

1) *Energy of cones*: At L2 we require two central ($|\eta| < 1.0$) cones having $E_T \geq 15$ GeV and 10 GeV respectively. These cuts are intentionally kept as much low as possible to not create a sizeable bias on the invariant mass distribution.

2) *Track-cone matching*: At L2 we have at our disposal tracks reconstructed by SVT [3] [4] tracker. To fully exploit information from XFT and SVT trackers, we build *hybrid tracks* looking for SVT tracks matching XFT stereo ones. The matching is performed on azimuthal angle ϕ and curvature c ($\Delta\phi < 0.02$ rad and $\Delta c < 0.0001$ cm $^{-1}$).

Hybrid tracks are then matched in $\eta - \phi$ plane to a central L2 jet ($\Delta R < 0.7$). We require at least 2 hybrid tracks matched to a L2 jet and once at least one match is found, we perform a further selection on parameters of hybrid tracks inside the cone.

3) *Impact parameter*: SVT, among other variables, provides impact parameter (d_0) measurement with a resolution of $35 \mu\text{m}$ for 2 GeV/c tracks comparable to the resolution obtained for offline reconstructed data. This has allowed to trigger with great success on B events since several years and now can open to the b -tracks inside a b -jet still based on tracks displaced from primary vertex.

The impact parameter of a track matched to the L2 jet is a very discriminant variable. In fig. 1 d_0 distribution is shown for signal and background. Tracks from b -jets have higher d_0 values with respect to light jet background.

4) *b decay length*: Considering $d_0 - \phi$ plane (fig. 2), tracks from b -jets are collimated along b -quark direction and a linear relation holds between their impact parameter and azimuthal angles:

$$d_0 \sim -R_b(\phi - \phi_b) \quad (1)$$

where R_b and ϕ_b are b decay length and azimuthal angle respectively. Each segment joining two points in $d_0 - \phi$ plane represents a 2-track displaced vertex and the opposite of its slope is an estimator of R_b . Real b -jets tend to have positive decay length (fig. 3), thus a cut on this variable can discriminate them from light background.

IV. OPTIMIZATION

Cut optimization on R_b and d_0 is performed aiming at the best compromise between efficiency on signal and background rate. For each cut on R_b , we scan $|d_0|$ values obtaining the family of curves in fig. 4. Each curve represents a cut on R_b and each point on the curve is a different cut on $|d_0|$. We choose to cut on $R_b > 0.2$ cm. This value provides efficiency on signal ranging from 11% to 17% (depending on d_0 cut) and a background rate going from 0.5% to 1.1%.

Once R_b is fixed, we look at the efficiency on signal and background varying the cut on d_0 (fig 5). A good

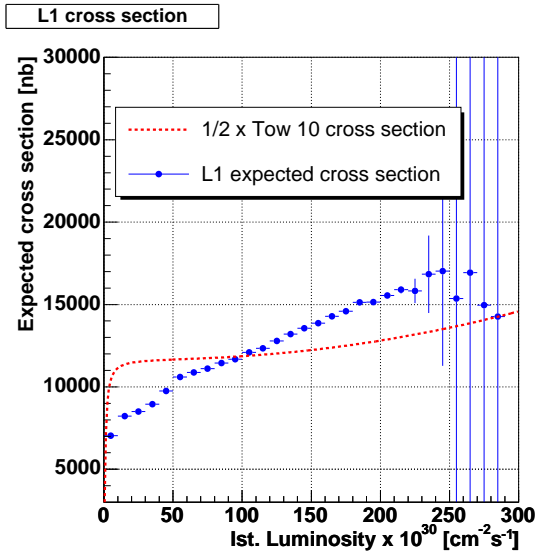


Fig. 6. L1 cross section (blue) as a function of instantaneous luminosity: L1 requirements allows to halve the cross section of Tower 10 (red), the trigger which collected data events used for our studies.

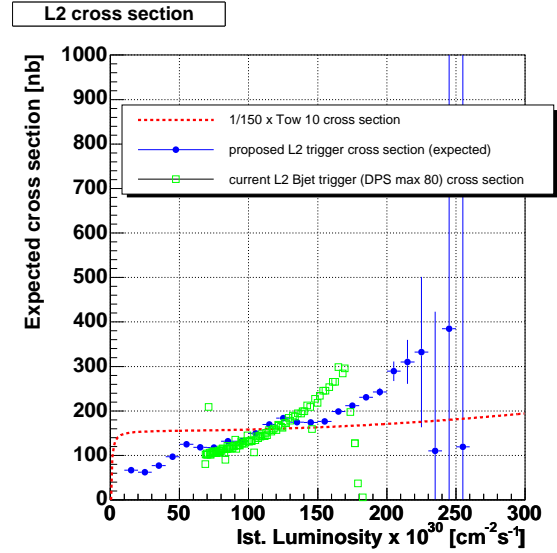


Fig. 7. L2 cross section (blue) as a function of instantaneous luminosity: the reduction with respect to Tower 10 cross section (red) is 1/150. Green curve is cross section of current L2 b -jet trigger, which is dynamically prescaled.

compromise between signal efficiency and background rate is $|d_0| > 160 \mu\text{m}$ which provides 14% eff on $H \rightarrow b\bar{b}$ events while rejecting 99.4% of background.

V. SUMMARY OF TRIGGER REQUIREMENTS

A. L1

- One $E_T \geq 10$ GeV trigger tower.
- Two XFT tracks with $\Delta\phi < 0.7$ rad.

B. L2

- Two cones with $E_T \geq 15$ and 10 GeV.
- At least 2 hybrid tracks matched to one of the leading cones.
- At least one 2-track displaced vertex with $R_b > 0.2$ cm.
- At least one track with $|d_0| > 160 \mu\text{m}$.

C. L3

L3 requirements have not been studied yet. The idea is to confirm L2 requirements with L3, offline-like, primitives.

VI. TRIGGER CROSS SECTIONS

Our goal is to develop a trigger which can run at high luminosity without saturating L2 trigger bandwidth. In fig. 6 and fig. 7 the L1 and L2 cross sections for our trigger are shown as a function of instantaneous luminosity. At L1 our cross section is half that of Tower10. Moving to L2, we obtain a cross section 150 times smaller than Tower10: at $L = 2.0 \times 10^{32} \text{ cm}^{-2} \text{ s}^{-1}$ cross section is 300 nb. These values, though preliminary, are very encouraging, especially when compared to the cross section of current L2 b -jet trigger (green curve) which is dynamically prescaled.

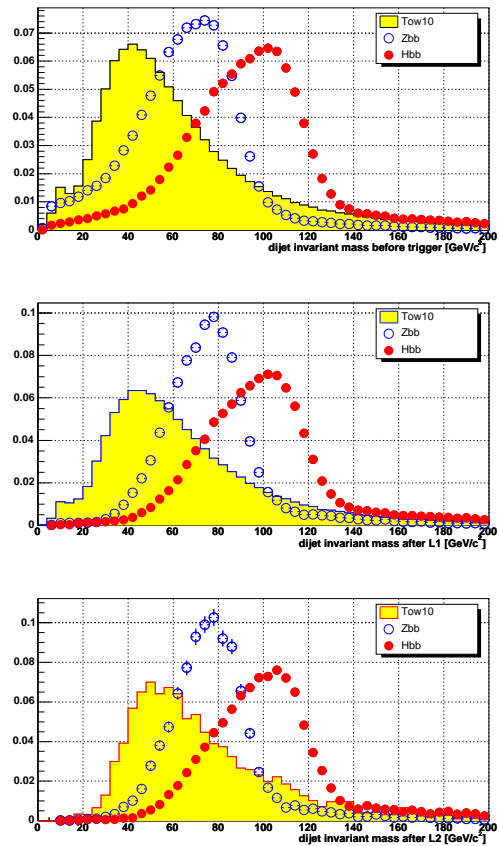


Fig. 8. Dijet invariant mass distribution before trigger, after L1 and after L2: signal dijet invariant masses are left almost unchanged by trigger requirements; background shape is slightly shifted towards greater energies but separation between peaks is not affected.

VII. CONCLUSIONS

We studied the feasibility of a new trigger able to perform online selection of b -jets up to luminosities greater than $2.0 \times 10^{32} \text{cm}^{-2} \text{s}^{-1}$. The trigger design exploits improved track and jet reconstruction available from recent trigger upgrades. Our algorithm is based on track-cone matching at L2 with loose requirements on jet energies, in order to minimize the effect on dijet invariant mass distribution. Trigger requests have almost no effect on signal dijet mass (fig 8), while background distribution is slightly shifted towards higher energies. Nevertheless separation between peaks is maintained.

We obtain a final efficiency on $H \rightarrow b\bar{b}$ of 14% and an acceptable cross section (300 nb at $L = 2.0 \times 10^{32} \text{cm}^{-2} \text{s}^{-1}$).

This trigger can also be used to select $Z \rightarrow b\bar{b}$ with an efficiency of about 4%.

Results presented in this paper are preliminary. The study of L3 requirements will be the subject of future work. Moreover, additional studies will be done in order to further reduce L2 trigger cross section at higher luminosity, as well as to meet L2 timing requirements.

ACKNOWLEDGMENTS

We thank the Fermilab staff and the technical staffs of the participating institutions for their vital contributions. This work was supported by the U.S. Department of Energy and National Science Foundation; the Italian Istituto Nazionale di Fisica Nucleare; the Ministry of Education, Culture, Sports, Science and Technology of Japan; the Natural Sciences and Engineering Research Council of Canada; the National Science Council of the Republic of China; the Swiss National Science Foundation; the A.P. Sloan Foundation; the Bundesministerium für Bildung und Forschung, Germany; the Korean Science and Engineering Foundation and the Korean Research Foundation; the Particle Physics and Astronomy Research Council and the Royal Society, UK; the Institut National de Physique Nucleaire et Physique des Particules/CNRS; the Russian Foundation for Basic Research; the Comisión Interministerial de Ciencia y Tecnología, Spain; the European Community's Human Potential Programme; the Slovak R&D Agency; and the Academy of Finland.

REFERENCES

- [1] A. Abulencia et al., FERMILAB-CONF-06-280-E and IEEE RT07 PS2002, Andrew Ivanov
- [2] Level-2 calorimeter Trigger Upgrade ar CDF, L. Sartori et al., IEEE Nuclear Science Symposium Conference Record and IEEE RT07 TDAQ-Trig09, Gene Flanagan
- [3] W. Ashmanskas, et al., Nucl. Instrum. Methods, A518, 532 (2004).
- [4] Annovi, A et al., Nuclear Science, IEEE Transactions on Volume 53, Issue 4, Part.2, Aug.2006 Pages:2428-2433
- [5] D.Acosta et al. (CDF Collaboration), Phys.Rev.D 71, 032001 (2005)
- [6] R.Blair et al. (CDFII Collaboration) the CDF RunII Detector Technical Design Report, 1996, FERMILAB-Pub-96/390-E